Near and Intermediate Field Evolution of A Negatively Buoyant Jet

Raed Bashitialshaaer[1,*] and Kenneth M. Persson[2]

[1]*Department of Water Resources Engineering, Lund University, John Ericsson no. 1, PO Box 118, SE-221 00 Lund, Sweden & Center for Middle Eastern Studies*

[2]*Department of Water Resources Engineering, Lund University, John Ericsson no. 1, PO Box 118, SE-22100 Lund, Sweden and Sydvatten AB*

Abstract: In this study, a mathematical model was developed to simulate the jet and plume behavior in order to determine the optimum discharge conditions for different scenarios. The model was divided into two sub-models, describing respectively the near and intermediate field properties of the discharge for different inclinations and bottom slope. The lateral spreading and electrical conductivity was also described through a generalization of measured data. The predictions of the model were compared with experimental data collected in lab as well as results obtained with a commercial software CORMIX. A Matlab code was also developed describing the lateral spreading and centerline dilution of buoyant jet and plumes for near and intermediate field was developed. The model produces results in acceptable agreement with data and observations, even though some improvements should be made in order to give the correct weight to the bottom slope parameter and to reduce the need for user calibration. This study has limited result for only 16% bottom slope and 30 degrees inclination. Concentration was improved with the bottom slope by 10% than the horizontal bottoms and improved by about 40% with bottom slope together with inclination of 30 degrees.

Keywords: Lab-scale experiment, Turbulent jet, Negative buoyancy, Desalination, Brine.

INTRODUCTION

1.1. General

The usage of sea water as a source for water supply (intakes) has constantly been increasing, due to the development of desalination processes. The desalination process brings as output fresh water from one side and brine water (outfalls) on the other side. The disposal of brines directly into the sea can increase the salinity level in the proximity of the output, alter the ecosystem equilibrium, and bring losses in efficiency of the desalination plant, if the sea water uptake is influenced by this change. The brine discharge devices are usually positioned at the lowest point of the receiving water which can be either ocean or deep water sea outfalls. The discharged fluid density is generally different from that of the surrounding, due to either different temperature or chemical composition. The resulting buoyancy forces can have a great effect on both the mean flow and mixing. Brine discharge from desalination plants is the common and best example; this type is the so-called negatively buoyant or dense discharges, which have relatively high-salinity concentrations.

A particular discharge should be considered as "shallow" or "deep" depending on the relative dynamic impact of this flow and recipients, notably its fluxes of momentum and buoyancy. In total 72 runs were performed at the Department of Water Resources Engineering (TVRL) laboratory at an appropriate scale to ensure turbulent jet behaviour. We are focusing in particular on releases where the initial vertical momentum flux of the discharge is in the opposite direction of the buoyancy generated momentum flux as the Boussinesq assumption is applicable.

1.2. Concept of Jet Flow

In general, there are three regions of the jet flow can in general be identified as: the near-field, the intermediate-field and the far-field flow. The near-field is the initial flow or development region (named the potential core for a top-hat exit profile); it is usually found within ($0 \leq x/d_0 \leq 6$). The far-field is the fully-developed region where the thin shear layer approximations can be shown (with appropriate scaling); jet flows generally become self-similar beyond ($x/d_0 \geq 25$) [1]. The intermediate-field, or transition region, lies between the near- and far-fields of the jet. Method of understanding mixing in intermediate-field or transition was well defined qualitatively by flow visualization e.g. [2 ,3]. In the intermediate region of a round jet there was only Reynolds dependence of shear stress distributions as shown in [4]. They used method of a stereo particle image velocity (PIV) system. The mean and fluctuating velocity curves were plotted for Re = 1,500; 3,000; 5,000.

It was possible to investigate the effects of turbulent energy on the initial development and large scale

*Address corresponding to this author at the Department of Water Resources Engineering, Lund University, John Ericsson no. 1, PO Box 118, SE-221 00 Lund, Sweden & Center for Middle Eastern Studies; Tel: +46462632730; Fax: +46462224435; E-mail: ralshaaer@yahoo.com

ISSN: 1814-8085 / E-ISSN: 1927-5129/12

instabilities of a round jet by placing grids at the nozzle outlet to alter the jet initial conditions because the grids causes small scale injection of turbulent energy [5]. The jet lateral spreading and consequent dilution at the bottom is of considerable practical importance in assessing the environmental impact of the effluent on the receiving water at the discharge point [6]. The behaviour of laterally confined 2-D density current has been considered in past but the number on 3-D study was very limited [7-9]. Hauenstein and Dracos proposed an integral model based on similarity assumptions, which was supported by their laboratory experimental data of the radial spreading of a dense current inflow into a quiescent ambient [10].

Previous studies mainly focussed on the separate analysis of near-field and intermediate-field properties of buoyant jets and plumes. Some hypotheses on how to connect the two different zones have also been proposed. Turner and Abraham were the first to analyse this kind of problem of a vertical negatively buoyant jet [11, 12]. Many investigations and experimental works has been previously done by several authors for the near-field of vertical and inclined dense jets [13-19]. They have proposed an empirical solution and theoretical expressions mainly for the maximum rise level and the centreline dilution. Many studies investigated the main properties of submerged jets using non-dimensional numbers and developed empirical relationships based on such numbers. The dense layer spreads in all directions at a rate proportional to the entrainment coefficient [20]. His result was obtained by flowing salt solution on a sloping surface in a tank of freshwater and his experimental result was based on three different inflow buoyancy fluxes on three angles of incline of 5°, 10°, and 15°. The starting salt concentration was constant at 4 g/l for all runs.

Akiyama and Stefan developed an expression for the depth at the plunge point as a function of inflow internal Froude number, mixing rate, bed slope, and total bed friction [21]. Cipollina *et al*. presented a model based on the conservation of mass, volume flux, momentum and buoyancy flux, describing the evolution of a buoyant jet in the near field of the discharge, validating the model against laboratory data [22]. Sanchez [23] developed a similar model, and for the model testing data collected in the laboratory were employed, as well as data from [22]. He employed a range of entrainment coefficients in the model obtained from previous studies. Christoudoulou described theoretically the main factors affecting near-, intermediate-, and far-field properties, suggesting appropriate length scales for each zone [6].

Baines *et al*. studied the entrainment of ambient water into buoyant jets through the laboratory experiments, describing the effects on this parameter from the geometry of the system and the presence of

Table 1: Dispersion Tanks with Different Sizes Used in Earlier Experiments

Previous study	Cross-section (m)	Depth (m)
Turner, 1966 [11]	0.45 x 0.45	1.40
Demetriou, 1978 [28]	1.20 x 1.20	1.55
Alavian, 1986 [20]	3.0 x 1.50	1.50
Lindberg, 1994 [29]	3.64 x 0.405	0.508
Roberts *et al*., 1997 [30]	6.1 x 0.91	0.61
Zhang & Baddour, 1998 [31]	1.0 x 1.0	1.0
Pantzlaff & Lueptow, 1999 [32]	D = 0.295	0.89
Bloomfield and Kerr, 2000 [33]	0.40 x 0.40	0.70
Cipollina *et al*., 2005 [34]	1.50 x 0.45	0.60
Jirk G.H., 1996, 2004, 2006 [35,36,37]	CORMIX, CorJet	
Kikkert *et al*. 2007 [38]	6.22 x 1.54	1.08
Papanicolaou & Kokkalis, 2008 [39]	0.80 x 0.80	0.94
Shao & Law, 2010 [40]	2.85x0.85	1.0
This study	1.50 x 0.60	0.60
	2.0 x 0.50	0.60

boundaries [24]. Bleninger and Jirka developed the software CORMIX to calculate jet trajectories and dilutions rates for general purpose applications in engineering projects [25, 26]. Suresh *et al*. investigated the lateral spreading of plane buoyant jets and how they depend on the Reynolds number, suggesting and demonstrating that a reduction of the spreading occurs with an increase in the Reynolds number [27]. Table **1** is the summary of different sizes that have been used for laboratory mixing tank dimensions (L x W x H) as found in literature.

1.3. Objective

The present study focuses on the discharge of the residue brine water and on the modeling of its evolution in space downstream the discharge area. The overall objective of this work is the investigation of the behavior of a negatively buoyant jet, and the following bottom plume ideally composed of brine water from a desalination plant, with focus on the lateral spreading (perpendicular to jet or plume axis) and the evolution of the salinity concentration on the centerline. This kind of analysis will help to find the most effective parameters influencing spreading and mixing, in order to design a proper discharge system. The detailed objectives can be summarized as to:

- Run a set of laboratory experiments, simulating discharge conditions in bench scale
- Develop a mathematical model to describe lateral spreading and centerline dilution of buoyant jet and plumes for near and intermediate field
- Find out possible correlation of measured values with non-dimensional numbers, e.g. densimetric Froude and Reynolds numbers
- Observe the effect of main parameters variation on spreading and dilution properties
- Calibrate the mathematical model with data collected in the laboratory, and test it on a different set of data
- Compare measured data and modeled data with simulation results obtained using the software CORMIX and Matlab programme

LABORATORY AND EXPERIMENTAL WORK

2.1. General Descriptions

The apparatus and major materials used in the experiments at the laboratory were named as water tanks, flow-meter, digital frequency-meter, digital conductivity meter, pump, pipes, valves, nozzles and nozzles' support, salt and dye (see Figure **1**). Five different tanks were used in the experiments; three small tanks for mixing tap water with salt and colour to obtain the salty water necessary to create the

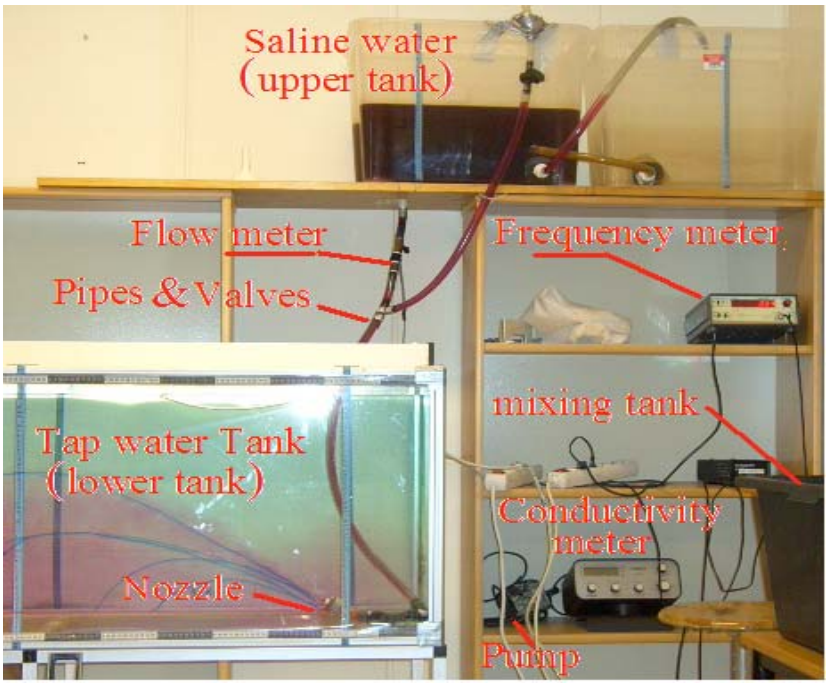

Figure 1: Terminology for experimental apparatus used (after [41]).

negatively buoyant jet and two large tanks used to fill with tap water and introduce the salty water with the dye to observe the jet inside it. The small tanks were made of plastics with capacities of about 45, 70 and 90 liters. The large tanks were in glass with capacities of about 500 to 600 liters. Their dimensions (L x W x H) were (150 x 60 x 60) and (200 x 50 x 60) each in centimetres.

Fine pure sodium chloride was used to create the saline water in the jet by mixing it with tap water. The water quantity was measured using a bucket and the salt was measured using a balance to obtain the correct salt concentration. A conductivity meter was used to measure the conductivity in the three different concentrations. The density measurement for the three concentrations presented in this study was found as 1025, 1039 and 1051 kg/m^3 for 4, 6 and 8% (40, 60 and 80 g/l) respectively. Each of the density was averaged of five different measurements from the weight method. Small differences in density measurements were reported between saltwater used in this study and natural seawater. The chemical composition of seawater is different from sodium chloride solutions, but the density varies only slightly compared with the pure sodium chloride solutions.

Potassium permanganate ($KMnO_4$) was used to colour the saline water. The dye colours the transparent water into purple by adding 0.1g/liter. The use of a purple jet was made to facilitate the observation of the behaviour of the jet in the tap water tank. The result of jar test for ($KMnO_4$) concentration showed that at 0.3 mg/l, the solution is still pink but at concentration of 0.195 mg/l no pink colour is visible.

2.2. Preliminary Measurements

Preliminary measurements were conducted after calibrating all apparatus in order to obtain reference data and to check if our measurement tools (i.e. flow meter, conductivity meter) were reliable and coherent with literature data. These measurements are flows, water salinity, density, and conductivity, diving information about water density and conductivity variation as a function of salinity at a constant room temperature of 20°C ±1°C. Each experimental run was characterized by a set of parameters, and the first step of each run was used to find the proper combination of parameter values. The parameters of interest were:

- Diameter of nozzle, d_o (4.8; 3.3; 2.3 mm)
- Initial jet angle, θ to the horizontal line (0; 30°)
- Bottom slope S_b (0; 16 %), the tank tilting
- Salinity of brine discharge S (4; 6; 8 %)

The two parameters submerged discharge angle θ and bottom slope S_b effecting the lateral spreading of the dense effluent. Lateral spreading is shown in Figure **2** in two dimensions x-axis and y-axis, in which b(x) was measured at three locations b_1, b_2 and b_3 at horizontal distances X_1, X_2 and X_3 for 20, 40 and 60 cm respectively. Similarly, EC(x) was also measured three times at the centreline of the x-axis. Nozzle parameters are denoted with zero (0) while ambient parameters are denoted as (a). The parameters along the centreline and flow direction are functions of x-axis and denoted as (x). In Figure **3**, the experimental strategies for submerged negatively buoyant for four cases are

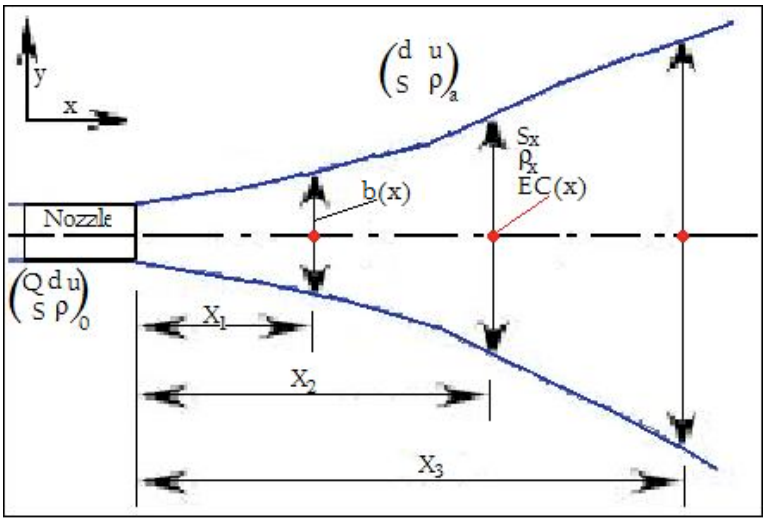

Figure 2: Plan view of lateral spreading measurements along the flow.

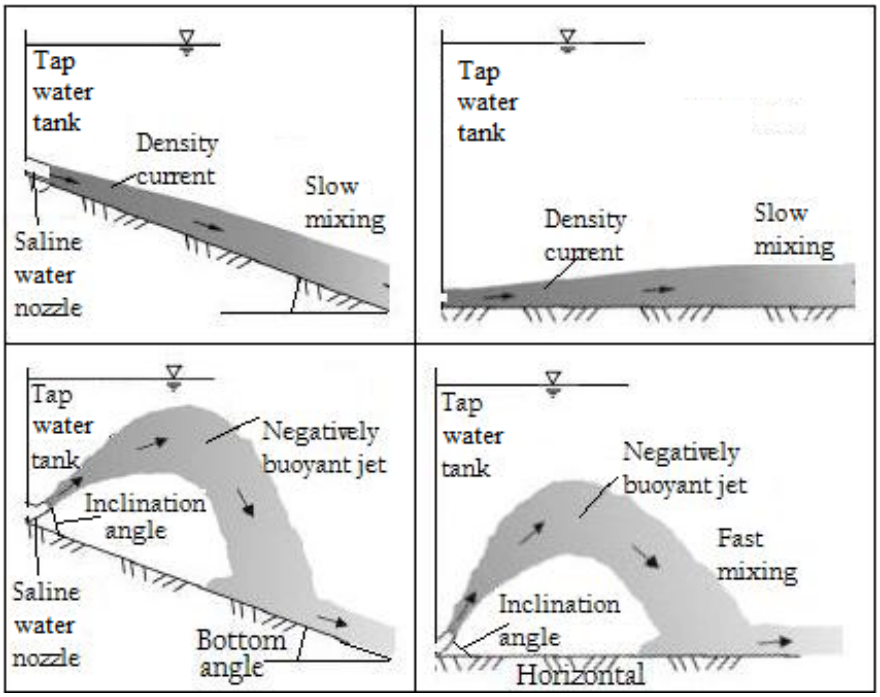

Figure 3: Experimental strategies for submerged negatively buoyant for four cases, changing in inclination and bottom angle (After: [42]).

Table 2: Experimental Results of Major Parameters for the Inclined Dense Jet

Run	Angle	S	d_0	S_b	$\Delta\rho_0/\rho_a$	Q_0	u_0	Fr_d	Spreading			EC during experiment			EC after experiment		
									(cm)			(μS/cm)			(μS/cm)		
	θ°	%	(mm)	%		(l/min)	(m/s)		b_1	b_2	b_3	EC_1	EC_2	EC_3	EC_1	EC_2	EC_3
1	0	4	2.3	16	0.027	0.68	2.73	111.3	15.5	32.5	43.5				1480	1586	1670
2	0	4	2.3	16	0.027	0.4	1.61	65.5	18.0	37.5	50.0				450	880	970
3	30	4	2.3	16	0.027	0.7	2.81	114.6	4.0	15.5	29.0				1070	1090	1130
4	30	4	2.3	16	0.027	0.48	1.93	78.6	5.0	16.5	31.0				580	920	940
5	0	4	2.3	0	0.027	0.62	2.49	101.5	6.0	12.5	27.0	3900	2500	2300	1400	1650	1850
6	0	4	2.3	0	0.027	0.4	1.61	65.5	7.5	14.5	29.0	3400	2300	1600	1480	1520	1530
7	30	4	2.3	0	0.027	0.57	2.29	93.3	5.0	11.0	16.0	3800	1900	1300	1200	1450	1400
8	30	4	2.3	0	0.027	0.34	1.36	55.7	6.0	13.5	19.5	3900	1300	1200	1180	1250	1210
9	0	4	3.3	16	0.027	1.3	2.53	86.3	6.0	19.0	36.0				1900	2000	2100
10	0	4	3.3	16	0.027	0.7	1.36	46.5	9.0	20.0	45.0				1100	1300	1600
11	30	4	3.3	16	0.027	1.3	2.53	86.3	5.0	9.0	31.0				1400	1500	1600
12	30	4	3.3	16	0.027	0.7	1.36	46.5	6.0	16.0	43.0				1100	1100	1200
13	0	4	3.3	0	0.027	1.01	1.97	67.1	6.0	16.5	30.0	4000	2600	2300	1800	2200	2200
14	0	4	3.3	0	0.027	0.6	1.17	39.8	8.0	21.0	33.0	3900	2700	2300	900	1300	1600
15	30	4	3.3	0	0.027	1.04	2.03	69.1	4.0	14.0	26.0	4500	2300	1900	1400	1400	1400
16	30	4	3.3	0	0.027	0.61	1.19	40.5	5.5	15.5	31.0	3900	2200	1400	1300	1350	1400
17	0	4	4.8	16	0.027	1.14	1.05	29.7	33.0	45.0	53.0				2500	2700	2900
18	0	4	4.8	16	0.027	0.65	0.60	16.9	26.0	37.0	50.0				403	394	416
19	30	4	4.8	16	0.027	1.13	1.04	29.4	39.0	46.0	53.0				1480	1550	1720

(Table 2). Continued.

Run	Angle	S	d_0	S_b	$\Delta\rho_0/\rho_a$	Q_0	u_0	Fr_d	Spreading			EC during experiment			EC after experiment		
									(cm)			(µS/cm)			(µS/cm)		
	θº	%	(mm)	%		(l/min)	(m/s)		b_1	b_2	b_3	EC_1	EC_2	EC_3	EC_1	EC_2	EC_3
20	30	4	4.8	16	0.027	0.68	0.63	17.7	35.0	43.0	51.0				480	670	967
21	0	4	4.8	0	0.027	1.24	1.14	32.3	10.0	24.0	35.5	5100	2900	2300	1600	2600	2900
22	0	4	4.8	0	0.027	0.79	0.73	20.6	13.0	27.0	37.0	3800	2600	2300	1500	1800	3100
23	30	4	4.8	0	0.027	1.3	1.20	33.8	7.5	20.0	30.0	5200	5100	2400	2100	2200	2300
24	30	4	4.8	0	0.027	0.72	0.66	18.7	10.5	25.0	36.0	4600	2100	1600	1900	2300	2300
25	0	6	2.3	16	0.041	0.77	3.09	104.2	16.0	25.5	38.0	4500	3200	2800	2200	2400	2600
26	0	6	2.3	16	0.041	0.53	2.13	71.7	22.0	32.0	42.0	3120	2000	1450	1200	1500	1750
27	30	6	2.3	16	0.041	0.77	3.09	104.2	11.0	20.0	32.5				1330	1400	1440
28	30	6	2.3	16	0.041	0.55	2.21	74.5	17.0	30.5	44.0				940	1060	1110
29	0	6	2.3	0	0.041	0.63	2.53	85.3	9.5	21.0	28.5	4500	3100	2600	1700	2500	2600
30	0	6	2.3	0	0.041	0.37	1.48	50.1	13.0	26.5	35.5	4100	2600	2400	600	1600	2000
31	30	6	2.3	0	0.041	0.6	2.41	81.2	5.0	11.0	14.0	3800	2500	1300	1500	1500	1500
32	30	6	2.3	0	0.041	0.41	1.65	55.5	7.0	10.0	16.0	3100	2200	1300	1400	1300	1400
33	0	6	3.3	16	0.041	1.19	2.32	65.3	25.0	38.0	46.0				2200	2300	2330
34	0	6	3.3	16	0.041	0.8	1.56	43.9	23.0	42.0	48.0				470	720	1600
35	30	6	3.3	16	0.041	1.07	2.09	58.7	21.0	33.0	42.0				1500	1650	1670
36	30	6	3.3	16	0.041	0.78	1.52	42.8	25.0	37.0	46.0				1260	1310	1320
37	0	6	3.3	0	0.041	0.93	1.81	51.1	13.0	22.0	32.5	6300	3300	3100	3000	3300	3500
38	0	6	3.3	0	0.041	0.63	1.23	34.6	15.0	25.5	37.5	5300	3600	1300	1100	2300	3100
39	30	6	3.3	0	0.041	1.04	2.03	57.1	5.5	16.0	22.0	5500	3300	1100	1900	2000	1900
40	30	6	3.3	0	0.041	0.58	1.13	31.8	7.0	19.0	25.5	4900	2000	1800	1800	1900	2200
41	0	6	4.8	16	0.041	1.43	1.32	30.8	40.0	48.0	53.0				2800	3200	3400
42	0	6	4.8	16	0.041	0.85	0.78	18.3	36.0	43.0	50.0				550	660	1300
43	30	6	4.8	16	0.041	1.17	1.08	25.2	31.5	43.0	53.0				2300	2500	2600
44	30	6	4.8	16	0.041	0.87	0.80	18.7	33.0	41.0	53.0				1205	1500	1700
45	0	6	4.8	0	0.041	1.27	1.17	27.3	13.0	26.0	33.5	7500	5000	3500	3300	3900	4300
46	0	6	4.8	0	0.041	0.89	0.82	19.1	21.0	30.0	40.0	4000	3600	2700	2400	3400	3600
47	30	6	4.8	0	0.041	1.01	0.93	21.7	15.0	23.0	32.0	6300	3000	2900	3200	3400	3400
48	30	6	4.8	0	0.041	0.87	0.80	18.7	17.0	26.0	35.0	5800	3100	2500	900	2800	3100
49	0	8	2.3	16	0.053	0.64	2.57	76.2	19.5	30.5	34.5	6500	4300	3900	2700	3100	3400
50	0	8	2.3	16	0.053	0.43	1.73	51.2	22.5	34.5	40.0	3400	2400	2000	1300	1900	2400
51	30	8	2.3	16	0.053	0.7	2.81	83.4	8.5	20.0	30.0	6000	3600	2300	1840	1900	2030
52	30	8	2.3	16	0.053	0.48	1.93	57.2	12.0	25.5	36.5	4900	1500	1000	860	1300	1400
53	0	8	2.3	0	0.053	0.67	2.69	79.8	11.0	19.5	30.0	6200	4300	2700	2100	3200	3500
54	0	8	2.3	0	0.053	0.42	1.69	50.0	14.5	23.5	32.0	5200	3000	2300	500	1200	2800
55	30	8	2.3	0	0.053	0.61	2.45	72.6	8.0	14.0	20.0	5200	2600	1800	2100	2200	2200
56	30	8	2.3	0	0.053	0.43	1.73	51.2	11.0	19.0	27.0	4400	1900	1300	1750	1810	2010
57	0	8	3.3	16	0.053	1.05	2.05	50.7	19.5	30.0	38.0	7500	5100	4500	3500	4300	4400
58	0	8	3.3	16	0.053	0.63	1.23	30.4	24.0	36.0	43.0	4500	3400	2400	1300	2100	2800

(Table 2). Continued.

Run	Angle	S	d_0	S_b	$\Delta\rho_0/\rho_a$	Q_0	u_0	Fr_d	Spreading			EC during experiment			EC after experiment		
									(cm)			(µS/cm)			(µS/cm)		
	θº	%	(mm)	%		(l/min)	(m/s)		b_1	b_2	b_3	EC_1	EC_2	EC_3	EC_1	EC_2	EC_3
59	30	8	3.3	16	0.053	1.15	2.24	55.5	11.0	21.0	28.0	4900	3000	2400	1900	2100	2300
60	30	8	3.3	16	0.053	0.67	1.31	32.4	21.0	36.0	42.0	3800	1400	1200	1300	1500	1600
61	0	8	3.3	0	0.053	1.05	2.05	50.7	20.0	32.5	40.0	9300	5400	3900	3100	3300	3500
62	0	8	3.3	0	0.053	0.7	1.36	33.8	28.5	40.5	47.0	6600	3200	2600	2300	3400	3700
63	30	8	3.3	0	0.053	1.06	2.07	51.2	9.0	23.5	36.0	7400	2900	1900	2500	2700	2700
64	30	8	3.3	0	0.053	0.71	1.38	34.3	16.5	30.0	42.0	5000	3400	2100	1400	2200	2300
65	0	8	4.8	16	0.053	1.21	1.12	22.9	28.0	37.5	39.0	7500	5200	4800	3500	4600	4800
66	0	8	4.8	16	0.053	0.91	0.84	17.2	32.0	40.0	48.0	4900	3500	3100	1100	2400	2700
67	30	8	4.8	16	0.053	1.43	1.32	27.1	25.0	35.0	44.0	6900	3100	2700	2700	3200	3400
68	30	8	4.8	16	0.053	0.97	0.89	18.4	29.0	39.0	50.0	5300	2000	1900	1700	2000	2200
69	0	8	4.8	0	0.053	1.17	1.08	22.1	27.0	36.5	35.0	7900	5500	6100	5600	6400	6600
70	0	8	4.8	0	0.053	0.9	0.83	17.0	36.5	43.5	48.0	6000	4300	5300	3400	3900	4400
71	30	8	4.8	0	0.053	1.25	1.15	23.7	23.0	32.5	39.5	8500	5800	4800	4500	5100	4800
72	30	8	4.8	0	0.053	0.89	0.82	16.8	27.0	39.0	46.5	4800	2400	2300	2600	3400	3600

presented, changing in inclination and bottom angle: (θ=0, S_b=16%; θ=0, S_b=0; θ=inclined, S_b=16%; θ=inclined, S_b=0). Each part of this figure was measured for 18 experiments with respect to three different salinities.

2.3. Data and Observations

Experimental data for inclined dense jets with major parameters for this study are listed (see Table **2**) for the 72 runs. The jet lateral spreading width b was measured at three distances 20, 40 and 60cm (see Figure **2**) and EC is the electrical conductivity reading at the same location of the three distances but only at the centreline; one set during the experiment in operation and another set after experiment stops.

MATHEMATICAL MODELLING AND DATA ANALYSIS

3.1. Dimensional Analysis

Brine discharge from a desalination plant is an example of denser fluid discharge to a stagnant ambient from a single port or a multiport at angle θ, with bottom slope S_b. This flow is conceptually divided into three connected regimes, the near-field, the intermediate field and the far-field Considering a negatively buoyant jet, the dilution at the impact point S_d in the near-field from a single port into a stagnant ambient comes with some assumptions. For the jet to retain its identity, the discharge angle should be small to avoid attachment to the bottom, or too large to avoid falling on itself [6]. From this assumption, the terminal minimum dilution at the impact point can be written as:

$$S_d = f(Q_0, M_0, B_0, \theta) \quad (1)$$

The jet is discharged at a flow rate Q_o through a round nozzle with a diameter d_o, yielding an initial velocity of u_o, with an inclination angle θ to the horizontal plane. Most previous studies employ the discharge as initial volume flux Q_o, kinematic momentum flux M_o, and buoyancy flux B_o as leading variables in the dimensional analysis. The three main parameters are given in the form as:

$$Q_o = \frac{\pi d_o^2}{4} u_o \quad (2)$$

$$M_o = \frac{\pi d_o^2}{4} u_0^2 \quad (3)$$

$$B_o = g\frac{\rho_o - \rho_a}{\rho_a} Q_o = g' Q_o \quad (4)$$

where g = acceleration due to gravity, and $g' = g(\rho_o - \rho_a)/\rho_a$ = the modified acceleration due to

gravity. The initial density of the jet is ρ_o and the density of the receiving water (ambient) ρ_a, where $\rho_o > \rho_a$, giving an initial excess density in the jet of $\Delta\rho = \rho_o - \rho_a$. The effect of the discharge is normally small and negligible, after simple dimensional analysis the initial dilution can be given by:

$$S_d = f_1(\theta, Fr_d) \quad (5)$$

where Fr_d is a Froude densimetric number defined as:

$$Fr_d = \frac{u_o}{\sqrt{g' d_o}} \quad (6)$$

A Froude number of 10 or larger simplifies the above equation to:

$$\frac{S_d}{Fr_d} = c(\theta) \quad (7)$$

Where the constant c is a function of inclined angle θ. Previously this constant was determined experimentally by many peoples e.g. [19] for 60^0 inclined angle as a value of c = 1.03, for the same angle [17] has an earlier estimation of c value of about 1.12.

In the description of the intermediate field lateral spreading of the dense plume along a mildly sloping bottom, one should take into account that at small slopes, the entrainment is small and negligible [7, 20, 43]. Therefore, the width of the plume should depend mainly on the buoyancy flux, the bottom roughness (drag coefficient C_d) and the geometrical characteristics of the problem [6]. Thus, the lateral spreading width b at the downstream at distance x can be written as:

$$b = f(x, b_0, B_0, S_b, C_d, g) \quad (8)$$

With simple dimensional analysis eq. (8) can be written as:

$$\frac{b}{b_0} = f_1\left(\frac{x}{b_0}, \frac{B_0}{g^{3/2} b_0^{5/2}}, S_b, C_d\right) \quad (9)$$

Alavian suggested that the terminal to initial width ratio b_n/b_0 is essentially independent of the slope for $5^0 \le S_b \le 15^0$, although the rate of approach to the normal state is faster for smaller slopes [20]. From the above statement the determination of the terminal width b_n for relatively small slopes (less than about 15^0), the explicit inclusion of S_b in, equation (9) can be omitted:

$$\frac{b_n}{b_0} \approx f_2\left(\frac{B_0}{g^{3/2} b_0^{5/2}}, C_d\right) \quad (10)$$

A power law form of equation (10) could be simplifies to:

$$\frac{b_n}{b_0} = K\left(\frac{B_0}{g^{3/2} b_0^{5/2}}\right)^a \quad (11)$$

Where $K = K(C_d)$. Equation (11) has been tested against limited experimental data in [20] and numerical results in [44]. They referred to a distance $x = 100b_0$, where the spreading width had not yet strictly reached a constant value, apparently due to the low drag coefficient employed. The value of the exponent was estimated in [6], as a = 0.183, while k exhibits an increasing trend with decreasing C_d.

3.2. Model Assumption

In this paper, mathematical modeling of the jet and plume evolution was essentially divided into two sub-models the near field and the intermediate field. The near field is the proximity of the nozzle, where jet and plume development is driven by the initial conditions; i.e. the initial momentum flux, volume flux, and buoyancy flux, and there is no interaction with the bottom. In the intermediate field, the buoyant jet essentially becomes a plume and it is interacting with the bottom. The main forces to be taken into account are bottom drag force and bottom slope effects. The "intermediate field" begins when the buoyant jet reaches the bottom. In order to develop a simple model describing the situation in the proximity of the discharge nozzle, some assumptions are made following [45]:

- Density differences are too small to affect inertia forces, but are important for the buoyancy force (the Boussinesque approximation). This assumption implies that the continuity equation can be described in terms of volume instead of mass
- Horizontal momentum of the jet is constant along the jet trajectory.
- Jet is symmetrical in a plane perpendicular to the jet axis.
- There is no influence from the boundaries of the receiving water.

- The section of the plume is not anymore round shaped but rectangular
- Plume is moving attached to the bottom; drag effect is taken into account by C_d.
- There is a linear relationship between concentration and density.
- Slope of the bottom is constant.
- There is a similarity for velocities and concentrations (or density deficit) in planes perpendicular to the jet axis (Gaussians distributions).

3.3. Validation of the Model

The validation of the model is one of the most important phases in the model building sequence. A completely independent set of parameters from the one used during the calibration must be used. For each experimental run three errors are calculated:

$$\varepsilon_{EC,i} = \left| \frac{EC_{model,i} - EC_{experiment,i}}{EC_{experiment,i}} \right| \quad (12)$$

$$\varepsilon_{b,i} = \left| \frac{b_{model,i} - b_{experiment,i}}{b_{experiment,i}} \right| \quad (13)$$

$$\varepsilon_i = \left| \frac{\varepsilon_{EC,i} - \varepsilon_{b,i}}{2} \right| \quad (14)$$

Where, $\varepsilon_{EC,i}$ is the error estimated in modeling of electrical conductivity (EC, µS/cm), in the i-th point of measurement (i = 0.2; 0.4; 0.6 m), $\varepsilon_{b,i}$ is the error in modeling of lateral spreading b, in the i-th point of measurement and ε is the overall average error, in the i-th point of measurement. The validation process was done considering the two different cases with and without the bottom slope as done before for the calibration. In Figure **4** the graphical visualizations of the error made in the modeling of the half width spreading and the concentration for the test without the bottom slope are reported. The best results are for the values closer to the trendline where the perfect correspondence between the model and the measures is. The sum of these two errors committed in the modeling is used to obtain an average error.

RESULTS AND DISCUSSIONS

4.1. Froude and Reynolds Number

Some limitations can be noted with the experimental setup, but these limitations were eliminated to a large extent by reproducing the experiments. The measurement of the lateral spreading, recorded on the bottom glass, was influenced by the visual impressions of the person who drew it, which created some difficulties to estimate the accuracy of the

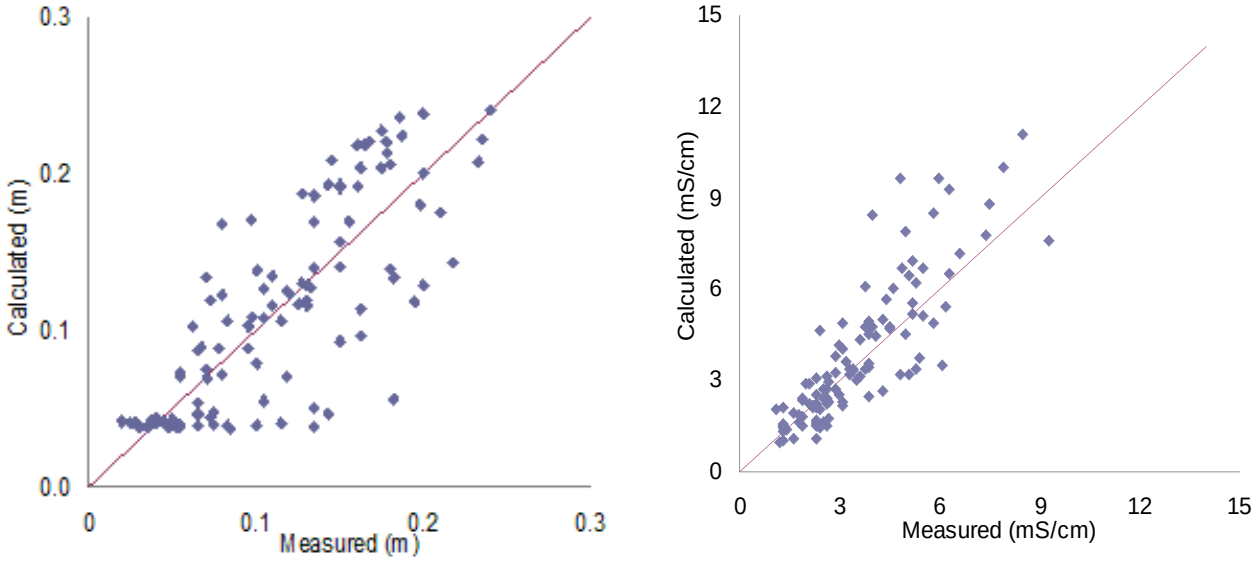

a **b**

Figure 4: a. Evaluation of the $\varepsilon_{b,i}$ error between measured and calculated half width spreading (b/2).
b. Evaluation of the $\varepsilon_{EC,i}$ error between measured and calculated Electrical Conductivity (EC).

measurements. An alternative methodology was applied by [27, 34] who used techniques based on image processing, capable of recording the jet with more accuracy, also at the lowest levels of tracer concentration. The measurement of electrical conductivity EC through a portable device is quite fast, but brings with it uncertainties concerning the exact location of the measurement point.

Also, the introduction of a probe during the test can disturb the flow regime downstream the measurement point. It was also difficult to estimate the error associated with the probe measurements. Non-dimensional lateral spreading measured at the plan view along the flow at horizontal distances 20, 40 and 60cm was drawn versus densimetric Froude and compared with Reynolds number figures. The figures exhibit the different behaviour of the measured data at the horizontal initial jet angle with and without bottom slope. The data vary with the densimetric Froude number in both cases with and without bottom slope while it exhibits the same trendline versus Reynolds number.

4.2. Comparisons with Matlab and CORMIX

The Matlab model could be applied successfully to model the experimental runs and the best results were

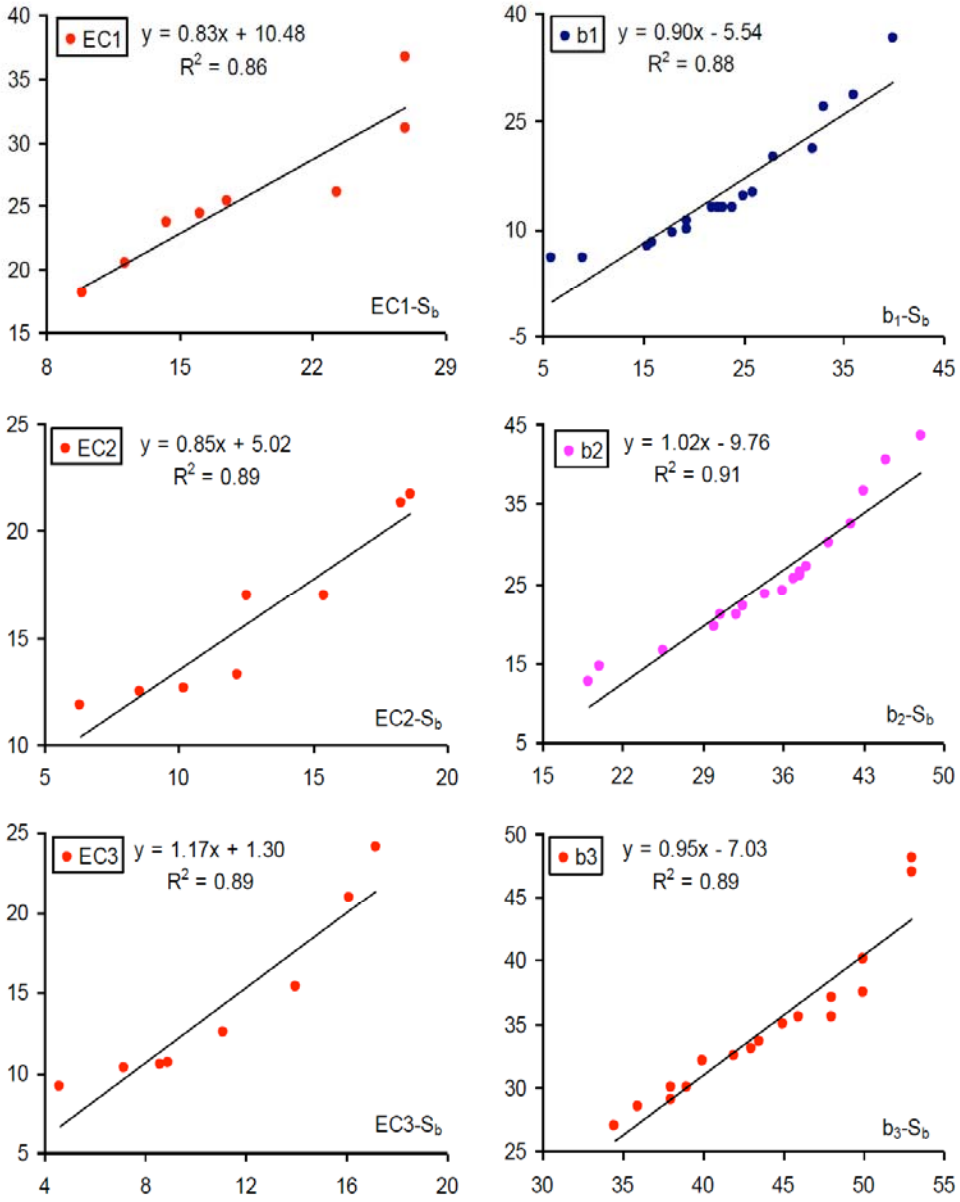

Figure 5: Electrical conductivity (EC as a ratio) and lateral spreading (b in cm) comparisons with and without bottom slope (S_b) at horizontal distances 20, 40 and 60cm.

obtained for the run without the bottom slope, as highlighted by the lower average error was previously calculated. The average error ε_i obtained in this case was around 28 %. Analyzing the experimental runs without bottom slope, an effort can be made to determine where more of the errors are found regarding the spreading and the concentration. Spreading values above the average are found for the runs with a salinity of 8 %, where an average error ε_i of 46 % was calculated. For all other salinities the average spreading error ε_i is around 28 %. From the comparison of the Matlab model with the experimental results is that the error for the lateral spreading is within the range of 30 % for all the measurements, slightly above the error without bottom slope.

Things became different considering the Electrical Conductivity, as a matter of fact the error made in this case is definitely larger and in particular for the measurements with θ equal to zero, where the error was around 60 %, twice the error made for θ equal to 30°. CORMIX was developed as software for hydrodynamic modeling of real (field) cases. In this study, the model was used to test its ability to describe results from small-scale laboratory experiments. However CORMIX merely provided exactly the same results in both cases; this unexpected behavior was revealed only when the values were compared to each other.

4.3. Bottom Slope Effects

Electrical conductivity ratio and lateral spreading compared with and without bottom slope at three horizontal distances 20, 40 and 60cm are presented in Figure **5**. The figures presented for electrical conductivity give an expression that there are small variations between flow on horizontal and with bottom slope. The correlations between the two cases are between 86-89%, which means the sloping bottom does not affect the flow regime. For the lateral spreading, it also showed that the correlation is 88-91%, much better than in electrical conductivity.

Normalized lateral spreading (b/d_0) and thickness of the dense layer (z/d_0) are drawn in Figure **6**, and compared for four cases at horizontal distances 20, 40 and 60cm along the x-axis with respect to inclined angle (θ) and bottom slope (S_b). Different comparison was made for interrelation between measured parameters to see the effect of initial angle and bottom slope. First we compare normalized lateral spreading in three different positions, inclined angle ($\theta = 0^0$) and bottom slope ($Sb = 0^0$) versus (θ = 30, Sb = 0); (θ = 0, Sb =16); (θ =30, Sb = 16). As it can be seen, for the lateral spreading all figures and trendline have shown good correlation and it is above 80% except one of them. Comparing the second part of Figure **6**, the normalized dense layer thickness showed that for two cases is not so good and it is below 70% and for one case with (θ = 30, Sb = 0) showed bad correlation which indicates that inclined and initial angle is much important than bottom slope.

The concept of dilution spreading up to the attainment of a normal state is correlated in normalized form with and without the bottom slope [6]. The estimation of lateral spreading and electrical conductivity comparisons will be useful in practical applications concerning the disposal of heavy industrial wastes or brines into coastal or inland waters. The result derived may allow us to understand and estimate overall dilution and final plume width up to the far field.

This estimation will be more useful in discharging brines from desalination plant. Based on the findings in

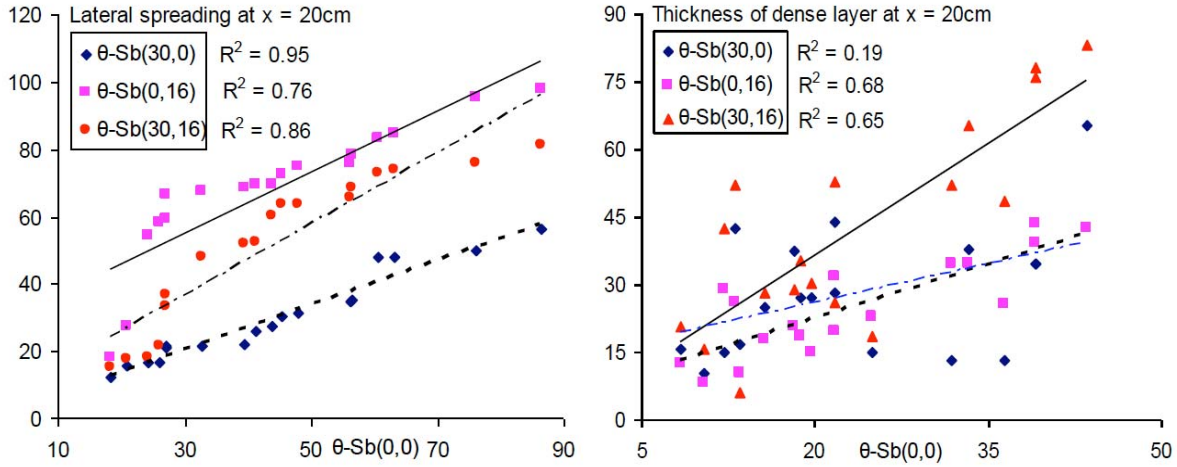

(Figure 6). Continued.

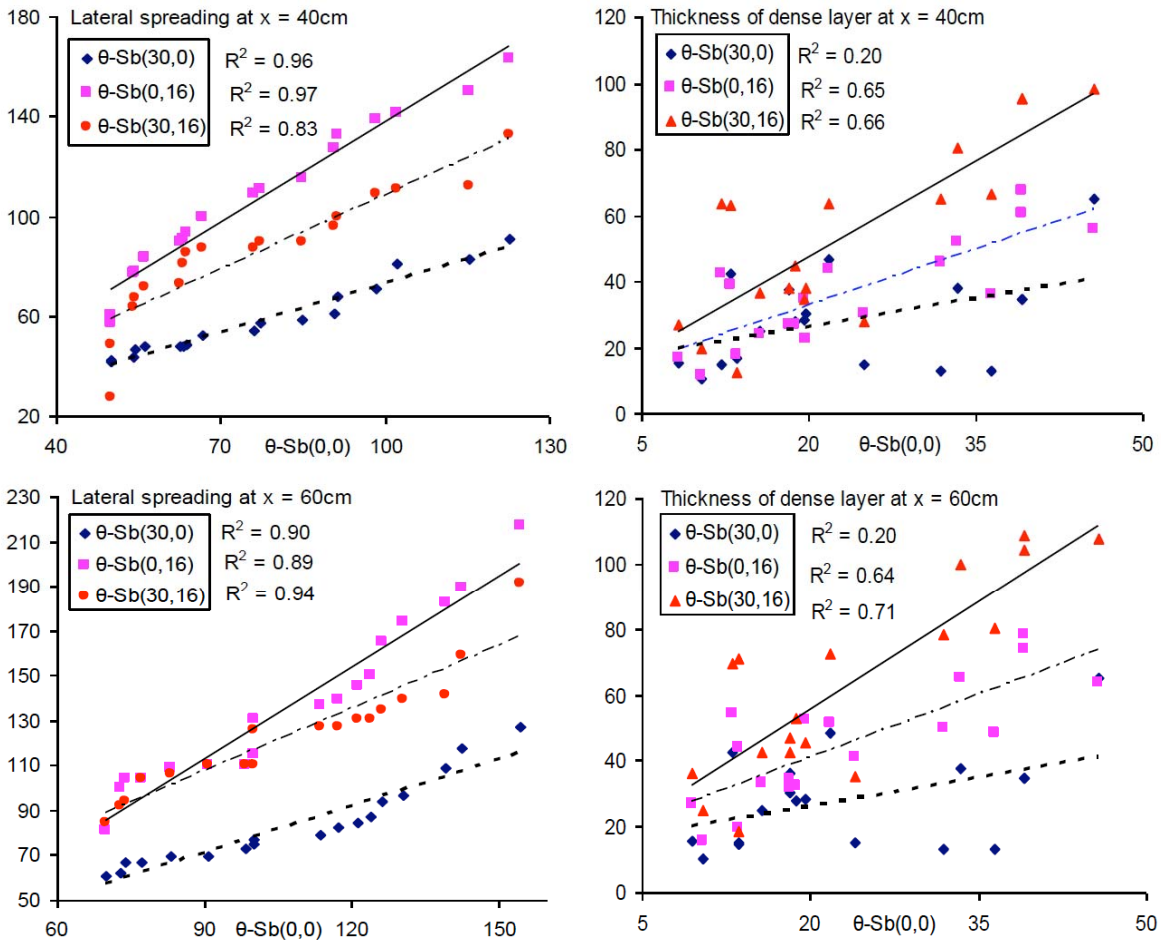

Figure 6: Normalized lateral spreading (b/d_0) and thickness of dense layer (z/d_0) comparison for four cases at horizontal distances 20, 40 and 60cm, with respect to inclined angle θ and bottom slope (S_b).

this study in the near- and intermediate the flow geometry depends on the angle of incline and the rate of supply of the dense fluid. After an initial spreading, the flow geometry becomes relatively constant with the horizontal distance down the slope [20]. For a given buoyancy flux, the normal layer width seems to weakly depend on slope.

The use of this study originally was made to be able to distinguish between different discharges at bottom slopes to the recipients including jet inclination angle. Desalination brine is the real case to consider in studying environmental impact and assessment when building new projects. In real life most of the recipient e.g. Seas and Oceans are naturally having bottom slope, this can be vary from coast to another. Therefore, an experimental result for concentration percentage that was measured at three distances along the flow was compared with and without bottom slope for densimetric Froude number smaller and larger than 40, as presented in Figure **7**. The concentration along the flow was improved by about 10% with the bottom slope for Froude number smaller than 40 as real discharge cases does. Thus, this type

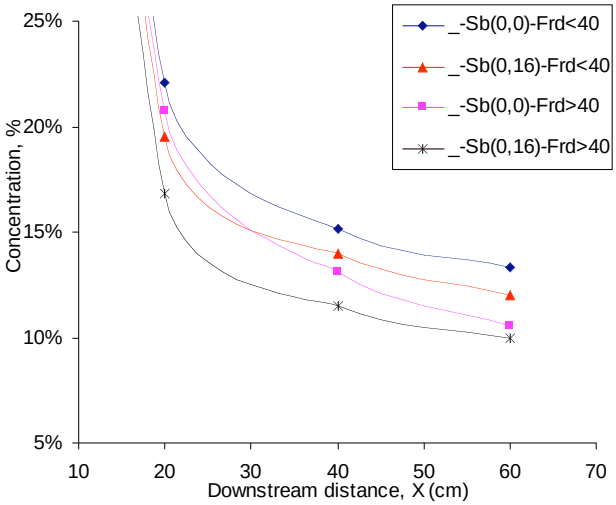

Figure 7: Concentration percentage along the flow with and without bottom slope.

of improvement can be used for brine discharge outlet to the recipients to minimize the concentration and let it dilute faster and goes farther. Another comparisons presented in Figure **8**, with and without bottom slope but this time including jet inclination angle of 30^0. It is also showed better improvement in the concentration of about 40% with bottom slope and inclination for Froude number smaller than 40, but small difference for Froude number larger than 40 which is not the case.

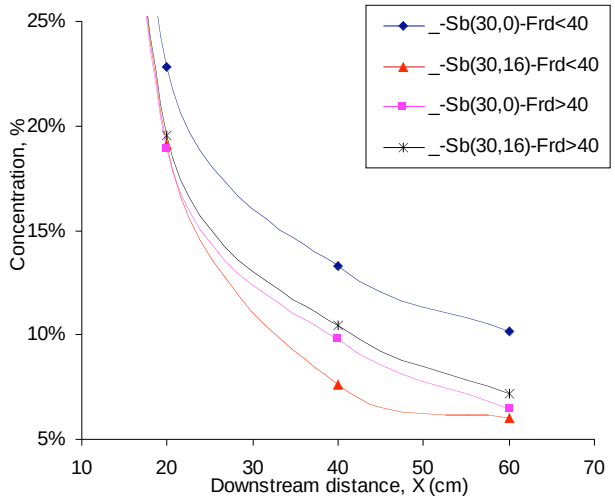

Figure 8: Concentration percentage along inclined flow with and without bottom slope.

CONCLUSIONS

The results achieved with the mathematical simulation model are satisfactory, considering the different behavior of the buoyant jet in the near and intermediate field. The Matlab model could be applied successfully to model the experimental runs and the best results were obtained for the run without the bottom slope, as highlighted by the calculation at lower average error. Non-dimensional analysis showed how the dilution and lateral spreading of brine discharge in the near and intermediate field is not related to the initial hydraulic properties, as represented by the densimetric Froude and Reynolds numbers. It is anyway important to underline that is not under discussion the fact that in the near field, the jet properties are strongly dependent by the initial condition, but in the present study the presence of near and intermediate field is considered together, without trying to divide the two different zones.

Based on the findings in this study in the near- and intermediate the flow geometry depends on the angle of incline and the rate of supply of the dense fluid. After an initial spreading, the flow geometry becomes relatively constant with the horizontal distance down the slope. For a given buoyancy flux, the normal layer width seems to weakly depend on slope. Concentration was improved with the bottom slope by 10% than the horizontal bottoms and improved by about 40% with bottom slope together with inclination of 30 degrees. The suggestion in the practical applications concerning desalination brines and similar discharge of heavy wastes is to have inclination and bottom slope together. This study has limited result for only 16% bottom slope and 30 degrees inclination, subject to further experimental study.

ACKNOWLEDGMENTS

Authors would like to thank Center for Middle Eastern Studies (CMES) at Lund University because the project was partly funded by them, primarily the experimental work. Also I would like to acknowledged Jacopo the two Master students from Italy Grazioli and Davide Noro for assistance in the valuable experimental and other work.

NOTATIONS

A = cross-sectional area

B_o = buoyancy flux the nozzle

b = lateral spreading

D = mixing tank diameter

d_o = nozzle diameter

Cc = centerline concentration

C_d = drag coefficient

EC = electrical conductivity

Fr_d = jet densimetric Froude number

g = acceleration due to gravity

g' = effective acceleration due to gravity

H = mixing tank depth

L = mixing tank length

M_o = momentum flux at the nozzle

Q_o = volume flux at the nozzle

PIV = particle image velocity

S = nozzle salinity

S_b = bottom slope

S_d = dilution at the impact point

u_o = nozzle velocity

W = mixing tank width

θ = initial jet angle

ρ_o = effluent density

ρ_a = ambient density

ε = error

REFERENCES

[1] Christopher, G.B.; Andrew, P. A Review of Experimental and Computational Studies of Flow from the Round Jet, Queen's University, Kingston, Ontario, Canada, INTERNAL REPORT No. 1, CEFDL. (2007/01),

[2] Dimotakis PE. The mixing transition in turbulent flows. J. Fluid Mech 2000; 409: 69-98. http://dx.doi.org/10.1063/1.864090

[3] Dimotakis PE, Miake-Lye RC, Papantoniou DA. Structure and dynamics of round turbulent jets. Phys Fluids 1983; 26: 3185-92.

[4] Matsuda T, Sakakibara J. In the vortical structure in a round jet. Phys Fluids 2005; 17: 1-11. http://dx.doi.org/10.1063/1.1840869

[5] Burattini P, Antonia RA, Rajagopalan S, Stephens M. Effect of initial conditions on the near-field development of a round jet. Expt Fluids 2004; 37: 56-64. http://dx.doi.org/10.1007/s00348-004-0784-4

[6] Christodoulou GC. Dilution Of dense effluents on a sloping bottom. J Hydraulic Res 1991; 29(3): 329-39. http://dx.doi.org/10.1080/00221689109498437

[7] Ellison TH, Turner JS. Turbulent entrainment in stratified flows. J Fluid Mech 1959; 9: 423-48. http://dx.doi.org/10.1017/S0022112059000738

[8] Benjamin TB. Gravity currents and related phnonmena. J Fluid Mech 1968; 31(2): 209-48.

[9] Simpson JE. Density Currents: In the environment and the laboratory, Ellis Horwood Ltd, Chichester, UK 1987.

[10] Hauenstein W, Dracos TH. Investigation of plume density currents generated by inflows in lakes. J Hydr Res 1984; 22(3): 157-79.

[11] Turner JS. Jets and plumes with negative or reversing buoyancy. J Fluid Mech 1966; 26: 779-92. http://dx.doi.org/10.1017/S0022112066001526

[12] Abraham G. Jets with negative buoyancy in homogeneous fluids. J Hydr Res 1967; 5: 236-48. http://dx.doi.org/10.1080/00221686709500209

[13] Anderson JL, Prker FL, Benedict BJ. Weakly depositing turbidity current on a small slope. J Hydr Res 1973; 28(1): 55-80.

[14] Chu VH. Turbulent dense plumes in a laminar cross flow. J Hydr Res 1975; 13: 253-79. http://dx.doi.org/10.1080/00221687509499702

[15] Pincince AB, List EJ. Disposal of brine into an estuary. J Water Pol Contr Fed 1973; 45: 2335-44.

[16] Shahrabani DM, Ditmars JD. Negative buoyant slot jets in stagnant and flowing environments, Ocean Engrg. Rep. No. 8, Dept. Civil Engrg., Univ. of Delaware, Newark, Del., U.S.A. 1976.

[17] Zeitoun MA, McHilhenny WF, Reid RO. Conceptual designs of outfall systems for desalination plants, Research and Development Progress Report No. 550, Office of Saline Water, United States Department of the Interior, 1970.

[18] Tong SS, Stolzenbach KD. Submerged discharges of dense effluent, R. M. Parsons Lab., Rept. No. 243, Mass. Inst. Of Tech, Cambridge, Mass., U.S.A. 1979.

[19] Roberts PJW, Toms G. Inclined dense jets inflowing current. J Hydr Eng ASCE 1987; 113(3): 323-41.

[20] Alavian V. Behavior of density currents on an incline. J Fluid Mech ASCE 1986; 112(1): 27-42.

[21] Akiyama J, Stefan HG. Plunging Flow into a Reservoir: Theory. J Hydr Eng ASCE 1984; 110(4): 484-99. http://dx.doi.org/10.1061/(ASCE)0733-9429(1984)110:4(484)

[22] Cipollina A, Bonfiglio A, Micale G, Brucato B, Dense jet modelling applied to the design of dense effluent diffusers. Desalination 2004; 167: 459-68. http://dx.doi.org/10.1016/j.desal.2004.06.161

[23] Sanchez D. Near-field evolution and mixing of a negatively buoyant jet consisting of brine from a desalination plant, Thesis work at Water Resources Engineering, Department of Building and Environmental Technology, Lund University 2009.

[24] Baines WD, Turner JS, Campbell IH. Turbulent fountains in an open chamber. J Fluid Mech 1990; 212: 557-92. http://dx.doi.org/10.1017/S0022112090002099

[25] Bleninger T, Jirka GH. Modelling and environmentally sound management of brine discharges from desalination plants, Accepted for EDS Congress, April 2007a, 22-25, Halkidiki, Greece.

[26] Bleninger T, Jirka GH. Towards Improved Design Configurations for Desalination Brine Discharges into Coastal Waters, IDA World Congress-Maspalomas Gran Canaria–Spain October 2007b, 21-26, REF: IDAWC/MP07-139.

[27] Suresh PR, Srinivasan K, Sundararajan T, Sarit DK. Reynolds number dependence of plane jet development in the transitional regime. Phys Fluids 2008; 20: 1-12. http://dx.doi.org/10.1063/1.2904994

[28] Demetriou JD. Turbulent diffusion of vertical water jets with negative buoyancy (In Greek), Ph.D. Thesis, National Technical University of Athens 1978.

[29] Lindberg WR. Experiments on negatively buoyant jets, with and without cross-flow, in: P.A. Davies, M.J. Valente Neves (Eds.), Recent Research Advances in the Fluid Mechanics of Turbulent Jets and Plumes, NATO, Series E: Applied Sciences, vol. 255, Kluwer Academic Publishers 1994; pp. 131-145. http://dx.doi.org/10.1007/978-94-011-0918-5_8

[30] Roberts PJW, Ferrier A, Daviero G. Mixing in inclined dense jets. J Hydr Eng 1997; 123(8): 693-99.

[31] Zhang H, Baddour RE. Maximum penetration of vertical round dense jets at small and large Froude numbers, Technical Note No. 12147. J Hyd Eng ASCE 1998; 124(5): 550-53.

[32] Pantzlaff L, Lueptow RM. Transient positively and negatively buoyant turbulent round jets. Exp Fluids 1999; 27: 117-25. http://dx.doi.org/10.1007/s003480050336

[33] Bloomfield LJ, Kerr RC. A theoretical model of a turbulent fountain. J Fluid Mech 2000; 424: 197-16. http://dx.doi.org/10.1017/S0022112000001907

[34] Cipollina A, Brucato AF, Grisafi, Nicosia S. Bench scale investigation of inclined dense jets. J Hydraulic Eng 2005; 131(11): 1017-22.

[35] Jirka GH, Doneker RL, Steven WH. User's Manual for CORMIX: A Hydrodynamic Mixing Zone Model And Decision Support System For Pollutant Discharges Into Surface Waters, DeFrees Hydraulics Laboratory School of Civil and Environmental Engineering, Cornell University 1996.

[36] Jirka GH. Integral model for turbulent buoyant jets in unbounded stratified flows, Part 2: Plane jet dynamics resulting from multiport diffuser jets. Environ Fluid Mech 2006; 6: 43-100. http://dx.doi.org/10.1007/s10652-005-4656-0

[37] Jirka GH. Integral model for turbulent buoyant jets in unbounded stratified flows, Part 1: The single round jet". Environ Fluid Mech 2004; 4: 1-56. http://dx.doi.org/10.1023/A:1025583110842

[38] Kikkert GA, Davidson MJ, Nokes RI. Inclined negatively buoyant discharges. J Hydraulic Eng 2007; 133(5): 545-54.

[39] Papanicolaou PN, Kokkalis TJ. Vertical buoyancy preserving and non-preserving fountains, in a homogeneous calm ambient. Int J Heat Mass Trans 2008; 51: 4109-20. http://dx.doi.org/10.1016/j.ijheatmasstransfer.2007.12.023

[40] Shao DW-K, Law A. Mixing and boundary interactions of 30^0 and 45^0 inclined dense jets. Environ Fluid Mech 2010; 10(5): 521-53.

[41] Bashitialshaaer R, Larson M, Persson KM. An Experimental Investigation on Inclined Negatively Buoyant Jets, Water 2012, 4. (Submitted to Water: Advances in Water Desalination).

[42] Bleninger T, Jirka GH, Weitbrecht V. Optimal discharge configuration for brine effluents from desalination plants, Proc. DME (Deutsche MeerwasserEntsalzung) - Congress, 04.-06.04 Berlin 2006.

[43] Britter RE, Linden PE. The motion of the front of a gravity current travelling down an incline. J Fluid Mechanics 1980; 99(3): 531-43.

[44] Tsihrintzisand VA, Alavian V. Mathematical modeling of boundary attched gravity plumes, Proceedings Inter. Symp. On Buoyant Flows, Athens, Greece 1986; pp. 289-300.

[45] Jönsson L. Receiving Water Hydraulics, Water Resources Engineering, Lund University 2004.

Received on 10-08-2012 Accepted on 08-09-2012 Published on 21-09-2012

http://dx.doi.org/10.6000/1927-5129.2012.08.02.43